Optical Properties of α-MnS†*

DONALD R. HUFFMAN‡ AND ROBERT L. WILD
University of California, Riverside, California
(Received 3 November 1966)

Optical characteristics of α-MnS have been determined from 0.02 to 14 eV. Single crystals were used for measurements above 0.05 eV. The shift with temperature of the ${}^6A_{1g} \rightarrow {}^4A_1$ crystal-field splitting peak is shown to be reasonably attributed to the effect of magnetic ordering. A broad weak band near 1 eV may be either an impurity band or the unallowed transition $Mn(3d^{++}) \rightarrow Mn(3d^{+})$. The absorption edge at 2.8 eV is explained as due to transitions from the wide $S^{2-}(3p)$ band to the narrow $Mn^{+}(3d)$ band. Two tiny peaks in the edge at 2.96 and 3.05 eV are suggested to be zero-phonon spin-orbit-split exciton peaks associated with this transition. High-energy absorption structure taken from Kramers-Kronig analysis of ultraviolet reflectance data are assumed to be associated with wide-band to wide-band transitions as in nonmagnetic compounds. A simple band diagram is suggested to explain the electronic transitions. The reststrahlen reflectance on a pressed powder was analyzed and the following parameters obtained: low- and high-frequency dielectric constants, 20 and 6.8; longitudinal and transverse optical mode frequencies, 320 and 185 cm^{-1}.

I. INTRODUCTION

SIMPLE compounds of the first transition series, such as the NaCl-structured oxides and sulfides, are of considerable interest in solid state physics because of diverse electrical, optical, and magnetic effects connected with their energy band structure. Little experimental information on these substances is available, however, because of difficulties in obtaining single crystals. Excellent crystals of α-MnS, a good representative of this type of compound, have been grown and their optical properties studied.

Manganese sulfide occurs in three crystal forms. The α form is a cubic NaCl-type structure with the distance between neighboring Mn or S atoms being 2.60 Å.[1] The β and γ forms are irreversibly converted to the stable α form upon heating.[2] In the α form (which will be understood for the rest of this paper), MnS shows a close similarity to the oxides MnO, CoO, and NiO. Antiferromagnetic ordering, which leads to anomalies in specific heat and magnetic susceptibility, occurs at the Néel point of 152°K.[3] Manganese sulfide shows a semiconductor type of increase of conductivity with temperature[4–6] although by simple energy band concepts the incomplete 3d shell should lead to metallic conduction. MnS is thus one of a category of low mobility solids over which controversy still exists as to whether "hopping-type" conduction occurs or not.[7]

The results presented in this paper are from an integrated set of measurements made to determine the important optical properties of MnS. Whenever possible the measurements were made on single crystals grown from carefully prepared and analyzed MnS powder.

II. SAMPLE PREPARATION

Single-crystal samples were grown from MnS powder prepared by precipitating Mn^{2+} ions from a $MnCl_2 \cdot 4H_2O$ solution with ammonium sulfide solution. Oxygen contamination was reduced by passing dry H_2S over the MnS powder as described by Archer.[8] Neutron activation analysis for oxygen content showed about 200 ppm of oxygen in the resulting powder.[9]

Single crystals were grown by the chemical-transport method with iodine as the carrier.[10] Conditions used were 5 mg/cm³ of iodine and temperatures of 850 and 450°C for hot and cold ends of the growth tube. Crystals grown under these conditions, in times varying from 8 to 36 h, usually occur in the form of platelets from 1 to 8 mm on a side, ranging from several microns to about 1 mm in thickness. The large faces are (111) planes which are seen to be highly perfect under examination by a metallurgical microscope. Occasionally a rod of 5 to 10 mm length with square cross section of approximately 1×1 mm is produced.

In infrared reflectance studies for which the single crystals are not large enough, polished ½-in.-diam pressed pills of MnS were used. The pills, pressed from finely ground MnS powder under a force of about 17 tons, had a density of about 0.92 of single-crystal density. Polishing was accomplished by using succeedingly finer grades of lapping compound followed by dry polishing on a paper covered polishing wheel with 3-μ powder.

† Submitted as a thesis in partial satisfaction of the requirements for a Ph.D. degree, University of California, Riverside, California.

* Work supported by the U. S. Air Force Office of Scientific Research.

‡ Present address: Physical Institute of the University, Frankfurt am Main, Germany.

[1] R. W. G. Wyckoff, *Crystal Structures* (Interscience Publishers, Inc., New York, 1963).

[2] P. Pascal, *Nouveau Traité de Chimie Minérale* (Masson and Cie., Paris, 1960), Vol. XVI, p. 949.

[3] D. R. Huffman and R. L. Wild, Phys. Rev. **148**, 526 (1966).

[4] C. F. Squire, Phys. Rev. **56**, 960 (1943).

[5] E. J. W. Verwey *et al.*, Philips Res. Rept. **5**, 173 (1950).

[6] R. R. Heikes, A. A. Maradudin, and R. C. Miller, Ann. Phys. (Paris) **8**, 733 (1963).

[7] A. J. Bosman and C. Crèvecoeur, Phys. Rev. **144**, 763 (1966).

[8] R. D. Archer and W. N. Mitchell, J. Chem. Phys. **39**, 250 (1963).

[9] Commercial analysis performed by General Atomics, San Diego, California.

[10] R. J. Nitsche, J. Phys. Chem. Solids **21**, 199 (1961).

III. MEASUREMENTS AND DISCUSSION OF RESULTS

A number of different techniques are available for determining optical parameters. The methods used to span the spectrum of MnS fall naturally into three divisions, each useful in a different wavelength region. From wavelengths of about 20 μ to 4500 Å, MnS is transparent enough for direct transmission measurements. At all shorter wavelengths down to 500 Å no measurable transmission occurs and ultraviolet reflectance techniques must be employed. In both of these ranges the platelet growth habit of the crystals proved to be ideal. In the infrared region, from about 30 to about 60 μ, the intense lattice absorption also precludes transmission measurements, and reflectance on a polished pill of pressed powder has been analyzed to determine the optical constants. The analysis and discussion of results for these three spectral ranges will be covered in the succeeding sections.

A. The Transparent Region

From photon energies of about 0.04 to 2.8 eV the absorption coefficient of MnS is less than 10^3 cm^{-1} and sufficient light is transmitted through the thin platelets for transmission measurements. Before such results can yield absorption coefficients, however, correction must be made for the reflectance loss at the surfaces. In this work a reflectance spectrum was independently determined for this purpose. In the transmitting region interference fringes arising from multiple reflections within the crystal were used to determine the index of refraction n from[11]

$$m\lambda = 2nd, \tag{1}$$

where d is the thickness, λ is the wavelength, and m is an integer. Assignment of the proper integer m was accomplished quite unambiguously by extending the measurements far enough into the infrared to reach $m=2$ or 3 for the thinnest samples. Thicknesses were determined by a Pratt and Whitney comparator, as used in accurate machine-shop measurements, and by a metallurgical microscope with a graduated reticle calibrated against standard distances on an engraved slide.

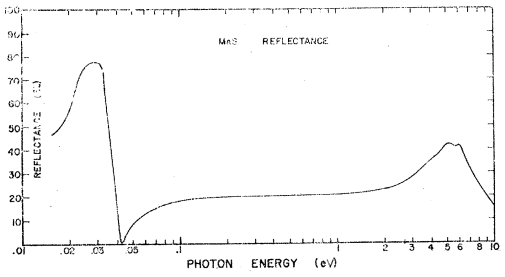

FIG. 1. Reflectance spectrum of MnS.

[11] T. S. Moss, S. D. Smith, and T. D. F. Hawkins, Proc. Phys. Soc. (London) **1370**, 776 (1957).

TABLE I. Variation of index of refraction with wavelength for α-MnS.

Wavelength (microns)	Index of refraction (n)
0.6	2.807
0.7	2.753
0.8	2.720
0.9	2.697
1.0	2.682
1.1	2.671
1.2	2.663
1.3	2.657
1.4	2.651
1.5	2.646
1.6	2.642
1.7	2.639
1.8	2.637
1.9	2.634
2.0	2.632
2.5	2.628
3.0	2.625
4.0	2.614
5.0	2.605
6.0	2.595
7.0	2.582
8.0	2.570
9.0	2.554
10.0	2.532
11.0	2.508
12.0	2.478
13.0	2.435

Having determined the fringe order and the thickness, an index of refraction was determined for the corresponding wavelength. Table I lists indices of refraction determined in this way. Accuracy of the values is limited by 0.5% uncertainty in thickness measurements. Spectral variation of n should be accurate to about 0.1% from 0.6 to 4 μ.

Reflectance values were determined from these indices of refraction by the Fresnel equation

$$R=\frac{(n-1)^2+k^2}{(n+1)^2+k^2}, \tag{2}$$

where n and k are the index of refraction and the extinction coefficient, respectively, defined as the real and imaginary parts of the complex index of refraction

$$N=n+ik. \tag{3}$$

Although details of the infrared and ultraviolet reflectance measurements will be presented later in this paper, it seems worthwhile to show the complete reflectance spectrum in Fig. 1. Agreement between different reflectance determining techniques in the small overlapping regions near 15 μ and near 6000 Å was found to be quite good.

With reflectance values so determined, optical absorption coefficients could be determined for crystals too thick to show interference effects from the transmission equation

$$I/I_0=(1-R)^2/(e^{\alpha d}+R^2e^{-\alpha d}), \tag{4}$$

where I/I_0 is the ratio of transmitted to incident light

TABLE II. Comparison of crystal-field peak energies from the present work and from Ford *et al.*[a]

Notation	This work measured (cm^{-1})	Ford *et al.* measured (cm^{-1})	Ford *et al.* calculated (cm^{-1})	Assignment
A	16 420	16 240	16 400	${}^6A_{1g} \rightarrow {}_a{}^4T_1$
B	19 398	19 440	19 290	${}^6A_{1g} \rightarrow {}_a{}^4T_2$
C	22 016	21 600	21 600	${}^6A_{1g} \rightarrow {}^4A_1; {}_a{}^4E$

[a] Reference 14.

intensity and α is the absorption coefficient which is related to k by

$$\alpha = 4\pi k/\lambda. \quad (5)$$

Equation (4) has been simplified from the general transmission equation[12] by elimination of the interference term and a term which is negligibly small in transmitting regions. Results for the absorption coefficients between strong absorption edges in the infrared and the ultraviolet are displayed in Fig. 2, plotted on an energy scale. Some gross qualitative optical properties are immediately seen. From the magnitudes of α involved, ($\ll 10^6$ cm^{-1}), one notices that between the two absorption edges near 0.05 eV and 3 eV apparently no intrinsic allowed optical transitions occur. The reason for the characteristic green color of MnS is obviously the region of relatively good transmission in the green at about 2.2 eV (5600 Å) situated between absorption peaks on either side. This has been generally recognized from previous work on MnS and similar work on MnO. It is not often appreciated, however, that pure α-MnS crystals are often deep red when thick enough for the green "window" to be highly absorbing compared to the greater transparency of the red. Beyond these qualitative comments there are several effects in the transmission region which warrant discussion. These are the three peaks in the visible at 2.0, 2.4, and 2.7 eV, the absorption edge near 2.8 eV, and the broad, weak absorption centered near 1 eV. These will be discussed in separate subsections.

Crystal-Field Splitting

Two experiments have previously revealed the three absorption peaks of MnS in the visible region. McClure[13] made an optical study of exchange interactions of Mn^{2+} ion pairs in ZnS:MnS mixed crystals and showed in his results an absorption spectrum of a pure MnS crystal at helium temperature. His results are identical with helium-temperature measurements of the present work down to the smallest of the multiple structure in the sharp peak. These details are therefore not displayed in this paper. The three peaks have been observed in a diffuse reflectance study of powder samples[14] of α, β, and γ MnS. Similar peaks have been observed in MnO[15] and in other manganese compounds.[16–18] From comparison with these results it is quite clear (as pointed out in Ref. 14) that the explanation for the three peaks in MnS lies in transitions between the ground state and excited states of the 3*d* levels of the Mn^{2+} ion which are split by the strong crystal field of the surrounding ions. Table II shows the peak positions of the three peaks taken at helium temperature from the present work compared with the measurements and assignments of Ford *et al.* The absorption band designated *C* is characteristically sharp in manganese compounds because of the insensitivity of the ${}^4A_1$–${}_a{}^4E$ level to changes in crystal field brought about by lattice vibrations. According to calculations of Koide and Pryce,[19] increasing covalency of the manganese compound results in lowering of this level and splitting of the originally degenerate ${}^4A_1$ and ${}_a{}^4E$ levels. According to their calculations, the energy of the sharp peak in MnS corresponds to a covalency parameter of about 0.2, at which value the ${}_a{}^4E$ state should be below the ${}^4A_1$ state. It therefore seems reasonable that the maximum absorption should be assigned to the transition ${}^6A_{1g} \rightarrow {}^4A_1$.

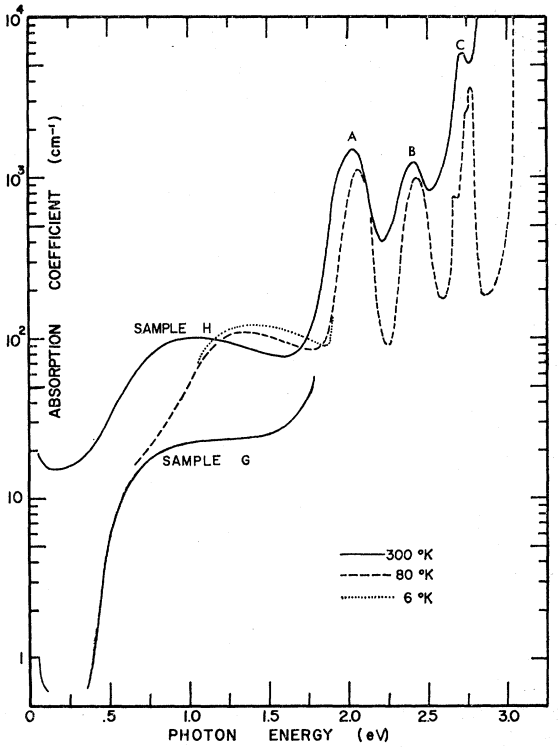

FIG. 2. Optical absorption spectra of MnS crystals.

[12] H. Y. Fan, Rept. Progr. Phys. **19**, 107 (1956).
[13] D. S. McClure, J. Chem. Phys. **39**, 2850 (1963).
[14] R. A. Ford, E. Kauer, A. Rabenau, and D. A. Brown, Ber. Bunsen Ges. Phys. Chem. (Germany) **67**, 459 (1963).
[15] G. W. Pratt and R. Coelho, Phys. Rev. **116**, 281 (1959).
[16] A. I. Belyaeva and V. V. Eremenko, Zh. Eksperim. i Teor. Fiz. **46**, 488 (1964) [English transl.: Soviet Phys.—JETP **19**, 330 (1964)].
[17] J. W. Stout, J. Chem. Phys. **31**, 709 (1959).
[18] I. Tsiyikawa and E. Konda, J. Phys. Radium **20**, 352 (1959).
[19] S. Koide and M. K. L. Pryce, Phil. Mag. **3**, 607 (1958).

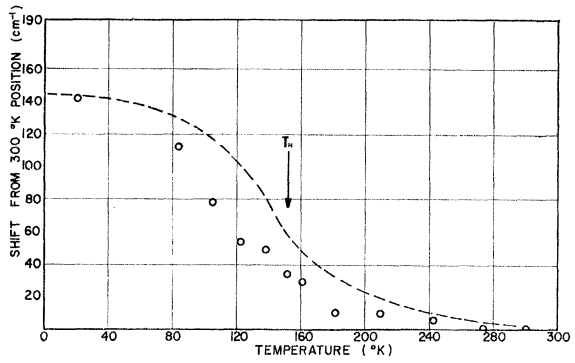

FIG. 3. Shift of the ${}^6A_{1g} \rightarrow {}^4A_1$ peak in MnS with temperature compared with a calculated shift. Open circles are data points and the dashed line is a calculated shift based on specific-heat data.

The width of the C peak itself is of some interest because it relates to the electronic conduction process in MnS. This width gives some measure of the upper bound of the combined width of ground and excited states, and therefore an upper bound on the width of the $3d$ band. It can be seen in Fig. 2 that the width of half maximum is about 0.1 eV. If the degeneracy of the excited state is actually split by covalency, part of the width of the bond must be caused by the unresolved splitting, and the actual width of the components may be 0.04 eV. In either case, it appears from optical evidence alone that the $3d$ band is rather narrow in MnS.

Since the temperature at which magnetic ordering occurs ($T_N = 152°\text{K}$) lies within the range of temperatures covered in optical absorption measurements, exchange related effects were sought. For this purpose line C is superior to A and B since it will be relatively unaffected by isotropic lattice parameter changes due to its independence of crystal field parameter Dq in first order. The sharpness of the peak also permits its position to be more accurately placed than is the case for the broader peaks. Wickersheim,[20] in fact, has mentioned that the width of most crystal-field peaks makes it impossible to observe the small exchange-induced effects except in a few cases like Mn^{2+} and Cr^{3+}. The position of the peak assigned to the ${}^6A_{1g} \rightarrow {}^4A_1$ transition was measured between helium temperature and room temperature. The shift of the line from the room-temperature position is shown for various temperatures by the open circles of Fig. 3.

In the case of small shifts such as this, it is necessary to consider the contribution from lattice distortion, even in cases where the energy of the transition is unaffected in first order. This has been attempted in several ways for the corresponding line of MnF_2.[17–21] Lacking information needed for either of these methods, we have simply calculated the exchange-induced shift and compared it with the observed shift.

The energy of the ith Mn^{2+} ion will be lowered by the antiferromagnetic ordering by

$$-\mathbf{S}_i \sum_j 2J_{ij}\mathbf{S}_j = U\,, \tag{6}$$

where S_i and S_j are the spin angular momenta of the ith and jth atoms, and J_{ij} is the usual exchange integral. S_i will be $\frac{5}{2}$ for the ground state. The shift of the excited state will be different because S_i becomes $\frac{3}{2}$ and the exchange integral is different. The ratio of the exchange energy in the two states can be estimated to a first approximation by a method due to Kanamori[17] and also used by Finlayson *et al.*[21] In this method the exchange is assumed to be proportional to the fractional occupancy of $d\gamma$ orbitals by spin components along the direction of antiferromagnetic alignment. According to this method the ${}^6A_{1g}$ ground state should be shifted by U, the ${}^4A_1$ state by $2/5U$, and hence the shift in energy of the ${}^6A_{1g} \rightarrow {}^4A_1$ transition should be $3/5U$. Now the exchange energy U does not change abruptly at T_N, the Néel temperature, in real antiferromagnets due to short-range order considerably above T_N and varying degrees of long-range order below T_N. The variation of U with temperature can be estimated, however, from the magnetic contribution to the specific heat. This fact was used by Stout to determine the magnetic energy U at the two temperatures of his optical data. Since we have recently reported specific-heat measurements,[3] we make use of these results. In order to extract the magnetic contribution from such data, however, it is necessary to separate out the lattice contribution. This can be a difficult matter.[22] Our method is to calculate the lattice contribution by Debye's theory using a reasonable value of Θ_D, the Debye parameter, estimated from room temperature infrared data. The rough Θ_D used was 300°K. The procedure used to estimate $E_m(T)$, the magnetic energy as a function of temperature, is summarized as follows:

1. A Debye specific-heat curve as a function of temperature was calculated for $\Theta_D = 300°\text{K}$.

2. The magnetic contribution was obtained as a function of temperature by subtracting the Debye curve from the experimental specific-heat values.[3]

3. A numerical integration of the magnetic specific heat was carried out from room temperature to 0°K to give $E_m(T)$ referred to the (almost) disordered state at room temperature. From this information U as a function of temperature is given by

$$\tfrac{1}{2}NU = E_m(T)\,, \tag{7}$$

$$U = 2E_m(T)/N\,, \tag{8}$$

where N is Avagadro's number and the $\frac{1}{2}$ keeps the exchange energy from being counted twice. The predicted

[20] K. A. Wickersheim, *Magnetism* (Academic Press Inc., New York, 1963), Vol. II, Chap. 7.

[21] D. M. Finlayson, F. S. Robertson, T. Smith, and R. W. H. Stevenson, Proc. Phys. Soc. (London) **76**, 355 (1960).

[22] J. W. Stout and E. Catalano, J. Chem. Phys. **23**, 2013 (1955).

optical shift from the 300°K position as a function of temperature is given from (8) as

$$\Delta E(^6A_{1g} \rightarrow {}^4A_1) = \tfrac{3}{5}(2E_m/N) = (6/5)E_m/N. \quad (9)$$

Results of this calculation are plotted in Fig. 3 as the dashed curve. In view of the uncertainties of this analysis, agreement of the shapes of the two curves and the total shift is excellent and perhaps fortuitous. In addition to the roughness of the approximation which was used to estimate the exchange shifts, a considerable uncertainty exists in the estimate of the lattice specific heat used to extract the magnetic energy. Because of these uncertainties it may be stated only that the total shift of the sharp line in MnS and the temperature dependence of the shift are reasonably accounted for by the exchange interaction.

Temperature shifts of the sharp line (C) in various compounds have been measured. Belyaeva and Eremenko[16] have shown a linear increase of the observed shifts with the Néel temperature for several of these compounds. The shift is indeed greatest for MnS, which has the highest Néel temperature of any of the compounds measured, but the linear relation of the shift to the Néel temperature is not obeyed. A corresponding shift of 150 cm^{-1} has recently been reported[23] for MnO between 77 and 295°K. Extension of these measurements to helium temperature would probably cause a greater total shift for MnO than the 150 cm^{-1} shift we have observed in MnS. This is somewhat surprising, since MnS has a higher Néel temperature (152°K) than MnO (120°K).

The Absorption Edge

A strong absorption edge near 2.8 eV at room temperature can be seen in Fig. 2. At low temperatures the edge shifts toward the violet by about 0.3 eV and sharpens up considerably. Measurements on the thinnest samples showed that the absorption coefficient rapidly exceeded 10^4 cm^{-1}, and analysis of ultraviolet reflectance confirms that the absorption coefficient is greater than 10^6 cm^{-1}. This suggests an intrinsic, allowed transition. Another small but perhaps significant feature of the edge is the presence of two tiny but clearly resolved absorption peaks in the spectrum of the thinnest sample at helium temperature. These extremely sharp peaks are located high on the absorption edge at 2.96 and 3.05 eV.

To aid in the interpretation of these optical data, it would be highly desirable to know the approximate relative positions of the Mn ($3d$) bands with respect to the S^{2-} band. A simple calculation based on free-ion ionization potentials and electron affinities, the Madelung potential, and a polarization correction can be made after the manner of Seitz,[24] and such as has been applied to NiO by Morin[25] and Van Houten.[26] Such a calculation suggests that the relative position of $3d^{2+}$ level may be a few electron volts above the center of the sulfur $3p$ band, with a $3d^{+}$ level somewhat higher than the $3d^{++}$. Since the electrons would occupy states through the $3d^{++}$ levels, two possible transitions need be considered. These may be represented by

$$Mn^{2+} + Mn^{2+} + h\nu \rightarrow Mn^{3+} + Mn^{+} \quad (10)$$

and

$$S^{2-} + Mn^{2+} + h\nu \rightarrow S^{-} + Mn^{+}. \quad (11)$$

The first reaction represents formation of a hole in the $3d^{2+}$ band and an electron in the $3d^{+}$ band. The second reaction represents the formation of a hole in the $3p$ band and an electron in the $3d^{+}$ band. The first reaction [Eq. (10)] is forbidden for electric dipole radiation since it takes place from the $^6F(3d^5)$ state to the $^5D(3d^6)$ state. The second reaction [Eq. (11)] is allowed. The 2.8-eV absorption edge is therefore ascribed to transitions from the wide sulfur band to empty $3d$ levels of manganese. Eagles[27] has developed a theory for optical absorption involving very narrow bands in ionic crystals. In discussing his results for wide band to narrow band optical transitions, Eagles suggests that exciton structure in the absorption edge will consist of a series of peaks at energies of $(E_e + p\hbar\omega_1)$ where E_e is the lowest exciton state, the p's are integers, and $\hbar\omega_1$ is the phonon energy. He suggests that individual phonon structure will probably not be resolved because of the broadness of the peaks, but absorption due to a process involving no emission or absorption of phonons will be a line absorption. It is therefore suggested that the two sharp peaks in the absorption edge of MnS may be such zero-phonon lines from the $3p \rightarrow 3d$ transition, the duality of the peaks being caused by spin-orbit splitting of the $3p$ valence band. Since sulfur is adjacent to chlorine in the Periodic Table, the spin-orbit splitting of the two should be similar. Considerable work on excitons in the alkali chlorides reveals splitting of exciton peaks by about 0.1 eV due to spin-orbit interaction.[28] The observed splitting of 0.09 eV is close enough to suggest the correctness of this explanation and to indicate further the participation of the $3p$ band edge in the 2.8 eV absorption edge.

The Near-Infrared Band.

Between the reststrahlen absorption and the crystal-field splitting peaks in the visible, there is a broad and comparatively weak absorption band apparently superimposed on a continuous background that rises steadily

[23] R. V. Pisarev and G. A. Smolenskii, Fiz. Tverd. Tela **7**, 2556 (1965) [English transl.: Soviet Phys.—Solid State **7**, 2064 (1966)].

[24] F. Seitz, *The Modern Theory of Solids* (McGraw-Hill Book Company, Inc., New York, 1940), p. 448.

[25] F. J. Morin, Bell System Tech. J. **37**, 1047 (1958).

[26] S. Van Houten, J. Phys. Chem. Solids **17**, 7 (1960).

[27] D. M. Eagles, Phys. Rev. **130**, 1381 (1963).

[28] H. R. Phillipp and H. Ehrenreich, Phys. Rev. **131**, 2016 (1963).

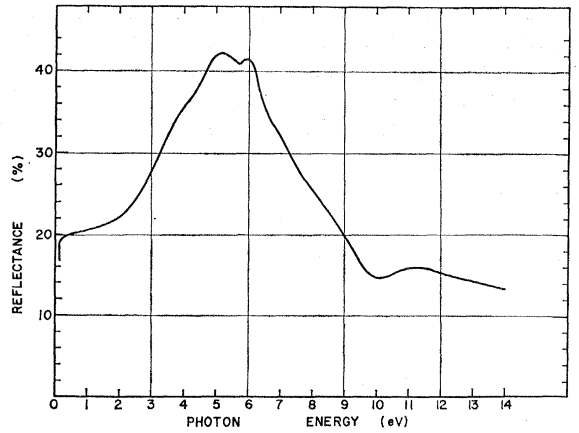

FIG. 4. High-energy reflectance spectrum of single-crystal MnS.

with increasing energy. Figure 2 shows the band for two samples, G and H. Sample H is more representative, since the three best samples of thickness 134, 277, and 577 μ reproduced the H curve in magnitude and in shape within the approximate limits of experimental error. Temperature variation of the data from sample G is given, since the peak is more easily separated from the background. The narrowing of the band and the shift to higher energy are similar to the behavior of F centers in ionic crystals[29] and to absorption by impurity-to-impurity excitation in semiconductors.[12] One possible explanation is, therefore, that the band is due to unknown, accidental impurities. In view of the relative position of d bands suggested in the preceding section, a second possibility is an excitation from the narrow $3d^{2+}$ band to the narrow $3d^{+}$ band. The width of the band would be due to multiphonon emission and absorption caused by strong coupling of the highly localized $3d$ electrons to the lattice. Such narrow-band to narrow-band absorption in ionic crystals has been discussed by Eagles.[27] Further measurements on thicker crystals, perhaps grown by a different method, are needed to establish the nature of the absorption mechanism with certainty in this weakly absorbing region.

B. Ultraviolet Reflectance

Because MnS crystals produced by the iodine transport reaction grow in the habit of platelets with very perfect, flat faces, they are ideal for reflectance measurements. The reflectance technique coupled with Kramers-Kronig analysis of the data has been used to extend the determination of optical constants into the far ultraviolet.

Experimental Method

Direct, almost-normal-incidence reflectance measurements were made with a McPherson model 235, 50-cm vacuum ultraviolet spectrometer. The dispersing element was a 600 line/mm grating blazed at 3500 Å. Two light sources were used. For the region from 6000 to about 3500 Å, a Sylvania Sun Gun incandescent lamp was mounted outside the entrance slit. From 3500 Å to all shorter wavelengths, the McPherson, Hinteregger type discharge lamp was used. In order to make the near-normal-incidence measurements without use of either a reference mirror or two different detectors, a device was constructed to permit movement of the sample in and out of the beam and to rotate the detector into either the incident beam or the reflected beam without disturbing the sample chamber vacuum. The photomultiplier tube was an RCA 1P28, which was coated with sodium salicylate phosphor for use below 1600 Å. The specular reflectance spectrum of MnS single crystals is given in Fig. 4. The actual angle between the incident beam and the normal to the crystal surface was about 6°. The reflectance values given are an average of values for the four most flawless crystals. Comparison of results for the several crystals shows agreement to within about 2% up to 4 eV, within 6% in the region of the main maximum from 4 to 7 eV, and perhaps higher in the region above 10 eV.

Data Analysis

Derivation of optical constants from the reflectance data was accomplished by the much used Kramers-Kronig analysis.[30] The phase shift θ was computed by numerical integration at 0.1-eV intervals throughout the region of reflectance data using an IBM 7040 computer. Since this type of analysis requires integration from zero to infinite energies, a reasonable extrapolation must be used to extend the data interval to infinity effectively. The technique proposed by Roessler[31] was employed in this work. In this scheme the extinction coefficient k is forced to be zero at two points in the

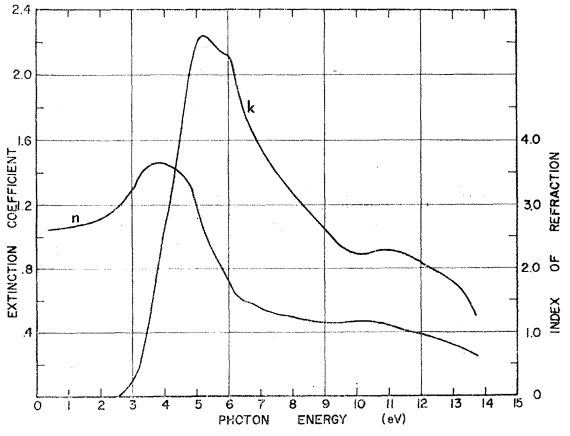

FIG. 5. Spectral dependence of the real and imaginary parts of the refractive index calculated from reflectance data.

[29] J. W. Schulman and W. D. Compton, *Color Centers in Solids* (Pergamon Press, Inc., New York, 1962), p. 54.

[30] F. Stern, in *Solid State Physics*, edited by F. Seitz and D. Turnbull (Academic Press Inc., New York, 1963), Vol. XV, p. 327.

[31] D. M. Roessler, Brit. J. Appl. Phys. **16**, 1119 (1965).

low-energy transparent region, and this condition is used to establish the high-energy extrapolation. Figure 5 gives the results for the real and imaginary parts of the index of refraction n and k. For completeness, the real and imaginary parts of the dielectric constant ϵ_1 and ϵ_2 and the absorption coefficient α, as computed from the data, are given in Figs. 6 and 7. These are related to n and k by

$$\epsilon_1 = n^2 - k^2, \tag{12}$$

$$\epsilon_2 = 2nk, \tag{13}$$

$$\alpha = 4\pi k/\lambda. \tag{14}$$

Discussion of Ultraviolet-Reflectance Results

The same general features are apparent in the various ways of presenting the results. The first main feature is the rise in ϵ_2, for example, beginning at about 2.8 eV to a peak near 4.8 eV which is apparently associated with the absorption edge observed in transmission. Near 5.8 eV, further absorption begins as seen clearly by the characteristic dip in ϵ_1. This is associated with the peak in absorption coefficient at 6.0 eV. From 6.5 to 10 eV a broad absorption band seems to be overlapping adjacent structure. Although some broad structure may be observed in this region, it is not believed that it should be strongly confirmed because of a very low light-source intensity in this region leading to greater uncertainty than elsewhere. From 10 to 14 eV, there is further broad structure, particularly noticeable in the absorption coefficient.

As already mentioned, the absorption beginning at 2.8 eV is considered to arise from charge transfer from the sulfur band to empty manganese $3d$ states. In addition to this band gap there will certainly be a higher "band gap" corresponding to excitations of electrons from the sulfur band to a $4d$-like band of manganese which should be quite broad. This band gap would correspond to that of the alkali halides, or more exactly, to the band gap of the alkaline-earth chalcogenides. Many of the alkaline-earth chalcogenides have the same cubic structure as MnS. In view of the similarities of

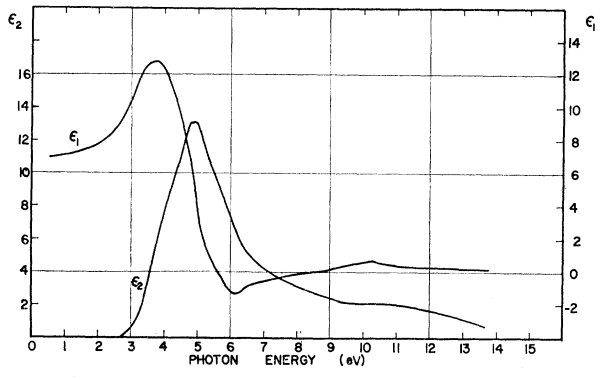

FIG. 6. Spectral dependence of the real and imaginary parts of the dielectric constant calculated from reflectance data.

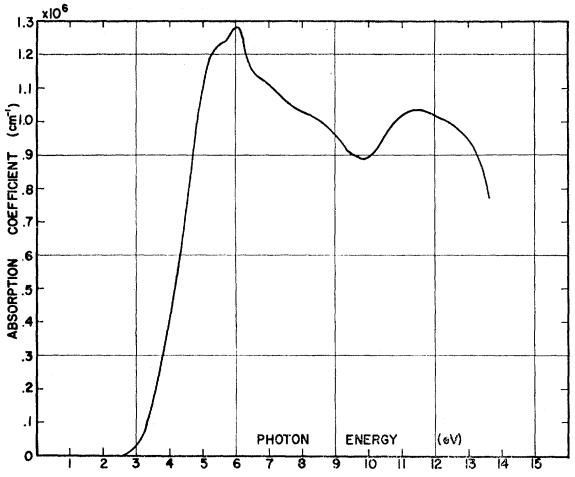

FIG. 7. Spectral dependence of the absorption coefficient calculated from reflectance data.

band structure found for crystals with the same or similar crystal structures,[32,33] the alkaline-earth chalcogenides might be expected to show absorption spectra similar to the NaCl-structured transition-metal chalcogenides, except for effects arising from the $3d$ band. Unfortunately, the information on such crystals is very scant. Enough measurements are available, however, to suggest that strong exciton processes just below the fundamental band gap are important in these crystals, although not quite so dominating as in the alkali halides. A rough correlation of apparent exciton peaks for these divalent compounds is given in Fig. 8, where the energy of the first exciton peak is plotted as a function of the inverse square of the lattice constant.[34–38] Whenever there is appreciable splitting of the sharp peaks, as expected from spin-orbit effects, the midpoint of the two peaks has been taken. Included in the correlation are unpublished data of Wild (EuS)[37] and Lawson (EuO, EuS, EuSe)[38] on apparent exciton peaks in the europium chalcogenides, which are insulating divalent compounds with NaCl-type structure. On the basis of the trend established in Fig. 8, MnS might be expected to show an exciton peak between 5 and 6 eV. Thus the relatively sharp absorption increase beginning at 5.8 eV may be due to excitons associated with transitions from the $3p$ band to a broad $4s$-like band of manganese. The broad absorption from 6.2 to 10 eV should then be assigned to band transitions associated with these bands. It is believed that the supposed exciton peak beginning at 5.8 eV

[32] J. C. Phillips, Phys. Rev. **136**, A1705 (1964); **136**, A1714 (1964); **136**, A1721 (1964).
[33] M. Cardona and D. L. Greenaway, Phys. Rev. **133**, A1685 (1964).
[34] R. J. Zallweg, Phys. Rev. **111**, 113 (1958).
[35] J. C. Kemp and V. I. Neely, J. Phys. Chem. Solids **24**, 332 (1963).
[36] E. Loh, Solid State Commun. **2**, 269 (1964).
[37] R. L. Wild (private communication).
[38] A. W. Lawson (private communication).

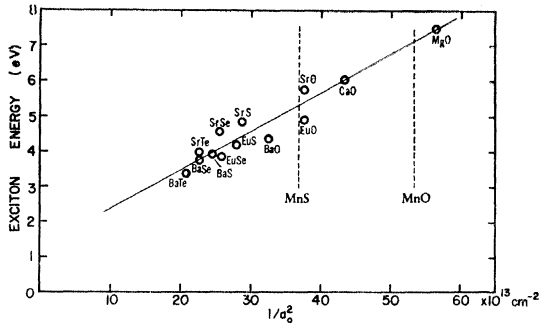

FIG. 8. Correlation of apparent exciton peaks with lattice constant a_0 for some divalent ionic crystals with NaCl structure. References for the data are as follows: Ba and Sr compounds, 33; CaO, 34; MgO, 35; EuS, 36; other Eu compounds, 37.

would be much clearer if it were separated from the lower-energy absorption band. Such a speculation could perhaps be checked if similar work were done on MnO. The decreased lattice constant should shift the band gap and exciton to higher energies, while absorption measurements have shown[15] that the lower-energy absorption edge occurs near the same energy as for MnS.

Lacking the guidance of any semblance of detailed band calculations pertaining to MnS, explanation of the higher-energy structures is likely to be even more speculative. However, in the light of Phillips's[32] review of the band structure deduced from numerous experiments on NaCl-structured alkali halides, a suggestion will be offered. If one assumes a free-electron model for the valence band, the next singularity in the density of states above the minimum of the conduction band may be expected to occur at the symmetry point L in the (111) direction at the Brillouin zone edge. A second critical point will be X in the (100) direction. The energy positions of these conduction-band critical points relative to the minimum point of the conduction band, assumed to be at the zone center Γ_1 is given by Phillips as

$$E_f(X)=\hbar^2/2ma^2=5.3 \text{ eV} \quad (15)$$

and

$$E_f(L)=3\hbar^2/8ma^2=4 \text{ eV}, \quad (16)$$

where the energies have been computed for the lattice constant a of MnS. Thus if the absorption band beginning near 6 eV is due to the onset of absorption at a minimum gap located at Γ, additional bands might begin at 10 and 11.3 eV. This could be an explanation for the 10–14 eV band.

C. Summary of Suggested Optical Transitions

The interpretation given for the effects noted in optical absorption spectra of the last two sections is summarized in Fig. 9. The basis for the figure is a band diagram with broad bands sketched by analogy with the bands of many NaCl-structured compounds surveyed by Phillips.[32] The suggested transitions in increasing order of their energy are as follows: (Numbers 2, 3, and 4 are based on helium-temperature data where the structure is clearer. The other transitions were measured at room temperature.)

(1) Near 1 eV—possible $3d^{++} \rightarrow 3d^{+}$ transitions between localized levels, with participation of many phonons. (This transition may be a nonintrinsic impurity effect.)

(2) 2.08, 2.46, and 2.78 eV—$3d$ crystal-field splitting transitions.

(3) 2.96 and 3.05 eV—tiny, spin-orbit-split exciton peak associated with the $3p \rightarrow 3d$, broad-band to narrow-band transition.

(4) 3.1 eV—$3p \rightarrow 3d$ broad-band to narrow-band absorption edge.

(5) 6.0 eV—possible $3p \rightarrow 4s$, broad-band to broad-band exciton peak assumed to be at Γ.

(6) 6.2–10 eV—$3p \rightarrow 4s$, broad-band to broad-band transitions.

(7) 10 eV—onset of transitions possibly at L in the (100) direction at the Brillouin zone edge.

D. Infrared Reflectance

Since there is considerable evidence that $3d$ electrons of MnS are in a very narrow band, coupling of these electrons to the lattice may be quite important, both optical and in electrical-conduction processes involving these electrons. Necessary parameters in the theories of slow-moving electrons and accompanying lattice polarization (polarons) are the low- and high-frequency dielectric constants ϵ_0 and ϵ_∞ and the longitudinal and transverse optical mode frequencies ω_0 and ω_1. These parameters have been measured in this work on MnS by measuring and analyzing the strong reflection band in the infrared, the reststrahlen band.

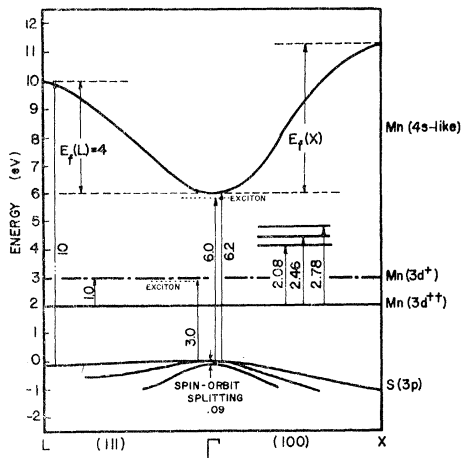

FIG. 9. Summary of suggested assignments for features in the optical absorption spectrum of MnS, based on a supposed band diagram.

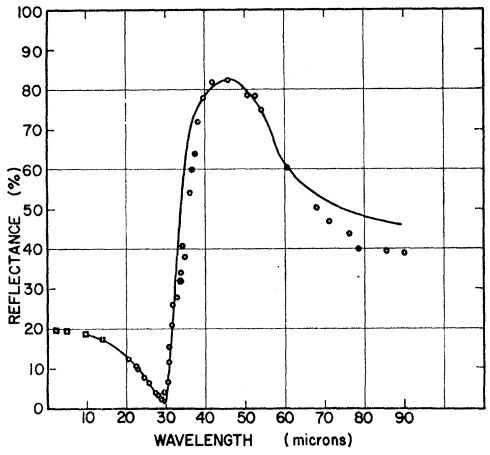

FIG. 10. Infrared reflectance of a polished powder sample of MnS compared with the best fit to a one-frequency dispersion calculation. Open circles and squares are data points and the solid curve represents the calculated curve.

The basic instrument used was the Perkin-Elmer model 301 spectrophotometer. Because of the small size of the single crystals compared to the beam of the spectrometer, measurements were made on a polished, pressed powder pill. In the absence of a reflectance attachment, the spectrometer was slightly modified for the reflectance measurements. A position on the second of two wheels inside the spectrometer which rotate reflection filters into the beam was used to mount the sample. Either the sample or a reference mirror could then be rotated into the beam for comparison. Since one of the principle elements for removing higher-order radiation from the diffracted beam had been eliminated, the other filter elements and wavelengths chosen for data points were carefully selected to give minimum higher-order radiation. The circles of Fig. 10 show the results of the measurements on a polished pressed powder pill of MnS from 20 to 90 μ.

These results were fitted to the phenomenological equations of Huang[39] for dispersion at a single frequency including a damping term. With the aid of an IBM 7040 computer, the four parameters ϵ_0, ϵ_∞, ω_0, and γ (the damping constant) were varied for the best fit to the data. The approximate sequence given by Spitzer[40] for varying the parameters for best fit was used. The results are indicated by the solid curve of Fig. 10. The values of the four parameters characterizing this curve are as follows:

$$\epsilon_0=20, \qquad \omega_0=185\ \text{cm}^{-1},$$
$$\epsilon_\infty=6.8, \quad \gamma/\omega_0=0.14.$$

It is seen from Fig. 10 that the greatest departure of the experimental points from the computed curve occurs at long wavelengths. If ϵ_0 were determined strictly from the long-wavelength reflectance, a considerably different value would be obtained. The procedure we have used, however, makes the determination of ϵ_0 more dependent on the width of the reflectance band which is less sensitive to errors in magnitude of the reflectance. Nevertheless, ϵ_0 contains an estimated uncertainty of $\pm 10\%$.

Two other parameters which are often of interest can now be determined for MnS. They are the longitudinal optical mode frequency given by the Lyddane-Sachs-Teller relation

$$\omega_1=(\epsilon_0/\epsilon_1)^{-1/2}; \quad \omega=320\ \text{cm}^{-1},$$

and the effective ionic charge[41]

$$e^*=0.76e.$$

ACKNOWLEDGMENTS

The authors would like to thank Professor J. Callaway for helpful discussions concerning the interpretation of the measurements. We also wish to thank Edward Middlemiss and Randolph Watts for the chemical preparation of MnS powder and Donald Decker for use of his crystal-growing furnace.

[39] K. Huang, Proc. Roy. Soc. (London) **A208**, 352 (1951).

[40] W. G. Spitzer, D. Kleinman, and D. Walsh, Phys. Rev. **113**, 127 (1959).

[41] B. Szigeti, Proc. Roy. Soc. (London) **A204**, 51 (1950).